7

CELL CULTURE MODELS FOR DRUG TRANSPORT STUDIES

IRINA KALASHNIKOVA, NORAH ALBEKAIRI, SHARIQ ALI, SANAALARAB AL ENAZY, AND ERIK RYTTING

Department of Obstetrics & Gynecology, University of Texas Medical Branch, Galveston, TX, USA

7.1 INTRODUCTION

High-throughput screening of pharmaceutical lead compounds can reduce the time, resources, and cost of identifying the most promising drug candidates at an early stage of the drug development process. Provided that a cell culture model can adequately predict permeability, biotransformation, or toxicity in a cost-effective manner, the use of such models can reduce the number of animal experiments that might have been required to narrow down a list of new compounds having the most preclinical promise. The elucidation of specific molecular mechanisms taking place at the cellular level represents another advantage of cell culture models [1].

This chapter will provide an overview of cell culture models that may be used to predict drug transport across relevant biological barriers. General considerations regarding the utility of such a model are discussed, followed by a brief description of physiological cell barrier properties and cell culture models that have been utilized or proposed to understand mechanisms of drug transport in the intestinal epithelium, the blood–brain barrier (BBB), nasal and pulmonary epithelium, ocular epithelial and endothelial barriers, the placenta, and renal epithelium. Examples of new developments regarding three-dimensional (3D) models are

Drug Delivery: Principles and Applications, Second Edition. Edited by Binghe Wang, Longqin Hu, and Teruna J. Siahaan.

also presented. Nevertheless, this is not a comprehensive overview of all possible cell culture models applicable to drug transport. Readers are referred to other sources for information on cell culture models of the skin and liver, for example see Refs. 2–6.

7.2 GENERAL CONSIDERATIONS

Cell culture models generally fall into one of two categories: primary cells and immortalized cell lines. Primary cultures are isolated from human or animal tissues, and cells of interest can be disaggregated by enzymatic or mechanical techniques (see Fig. 7.1) [7–9]. Cells capable of proliferation can be removed and redistributed onto new cell growth surfaces as a subculture. Additional subculturing (passaging) of cells can give rise to a cell line. Most primary cell cultures are not stable after a certain number of passages, and some will not proliferate at all. Senescence of the cell line can be caused by shortening of telomeres on the chromosomes. Upon reaching a critical telomere length, the cells will not continue to divide. Accordingly, transfection of the telomerase gene hTRT may be one means to produce an immortalized cell line [9]. Although immortalized cell lines can be generated by chemical or viral methods, some (often malignant) cells are spontaneously continuous [10].

Although immortalized cell lines are generally easier to work with, primary cells have certain advantages. In comparison to immortalized cell lines derived from malignant cells, primary cultured cells may be more representative of normal cell behavior *in vivo*. A major disadvantage of primary cell culture is the need for repeated isolation procedures due to the fact that most primary cells cannot be continuously subcultured to a substantial cell passage number. Differences in isolation conditions or heterogeneous tissue sources can lead to large variability in results obtained using

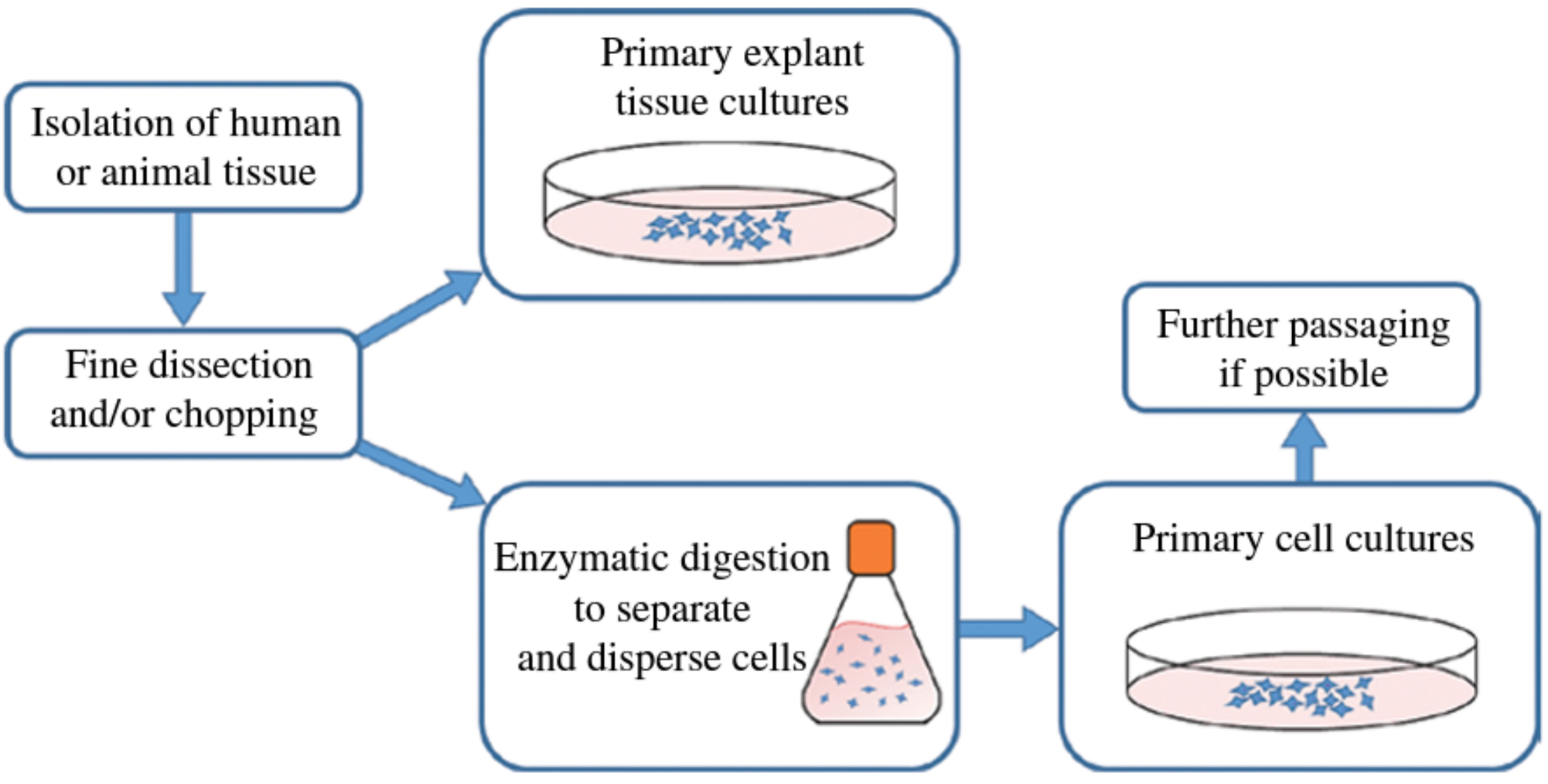

FIGURE 7.1 General methods for establishing primary explant tissue cultures or primary cell culture models isolated from human or animal tissues.

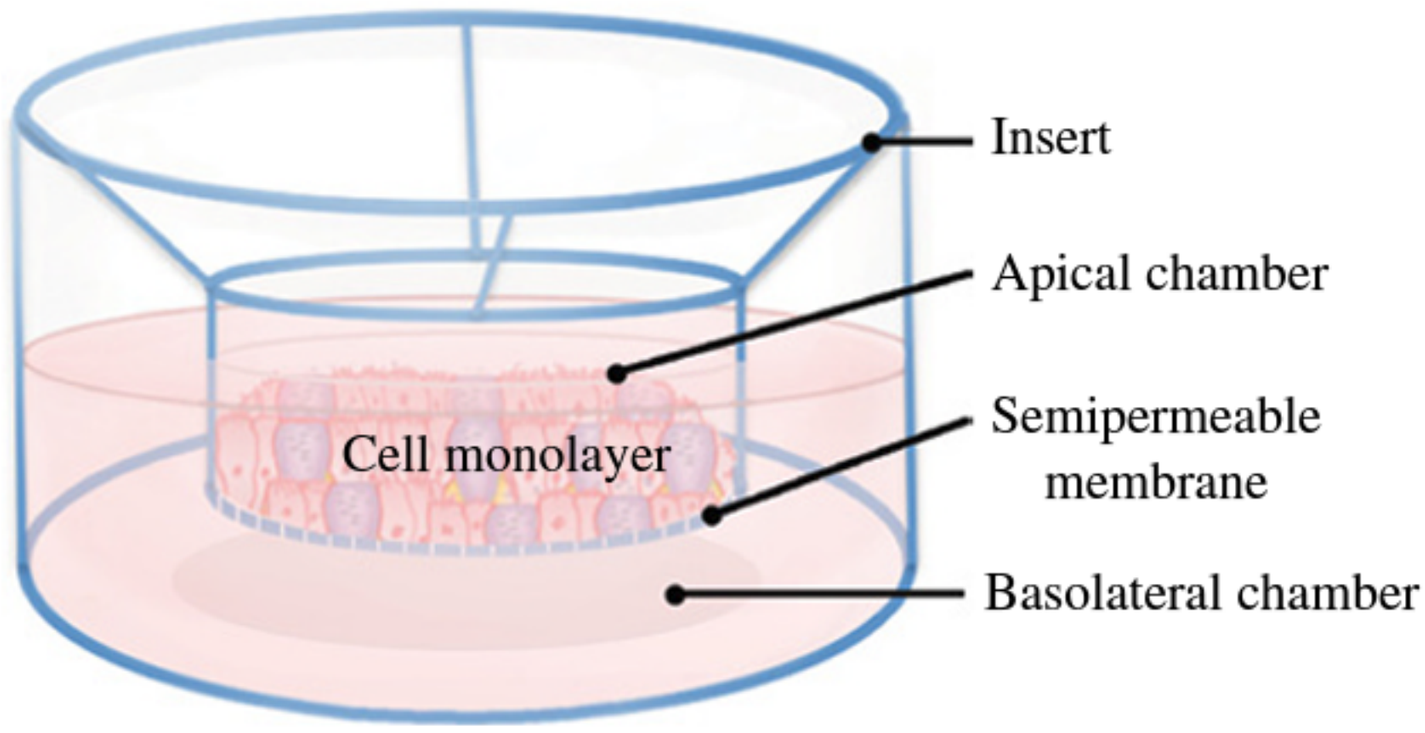

FIGURE 7.2 Inserts with semipermeable membranes can be used to study directional drug transport across cell monolayers. Samples can be taken from both the apical and basolateral sides of the cells.

primary cells. Although immortalized cell lines are more convenient to maintain, the abnormal nature of cell lines derived from malignant sources may limit the extrapolation of some data to normal cell populations. For example, certain immortalized cell lines may not express all relevant transporters [11]. Although the homogeneous nature of an immortalized cell line may lead to a smaller degree of variability in one's experimental results, it is important to note that from a pharmacogenetic standpoint, an immortalized cell line represents $n = 1$ individual and, therefore, cannot reflect the genetic variability of a population as well as might be achieved by isolating multiple sets of primary cells [12].

A number of criteria should be taken into account when selecting an appropriate model. For example, in addition to the aforementioned general advantages and disadvantages of primary versus immortalized cell lines, one should consider the passage number of the cell line and any associated limits on cell line stability, the suitability of the cell model to reflect *in vivo* barrier properties, reproducibility, the ease with which transport studies can be conducted, and the expression of relevant transporter proteins [1, 13]. A number of experimental set-ups permitting the feasibility of drug permeability studies across a cell monolayer have been described previously [1, 14, 15]. One example is the Transwell® insert, depicted in Figure 7.2. A comprehensive discussion of considerations for the selection of an appropriate experimental transport system—namely, cell type, matrix, filter support, medium or buffer composition, stirring, solute properties, and assay conditions—is provided by Ho et al. [16].

7.3 INTESTINAL EPITHELIUM

7.3.1 The Intestinal Epithelial Barrier

Assessing the absorption and bioavailability of orally administered drugs is an important step in drug development. By using cell culture models to understand the oral bioavailability of drugs, costs are significantly reduced and, as a result, drugs

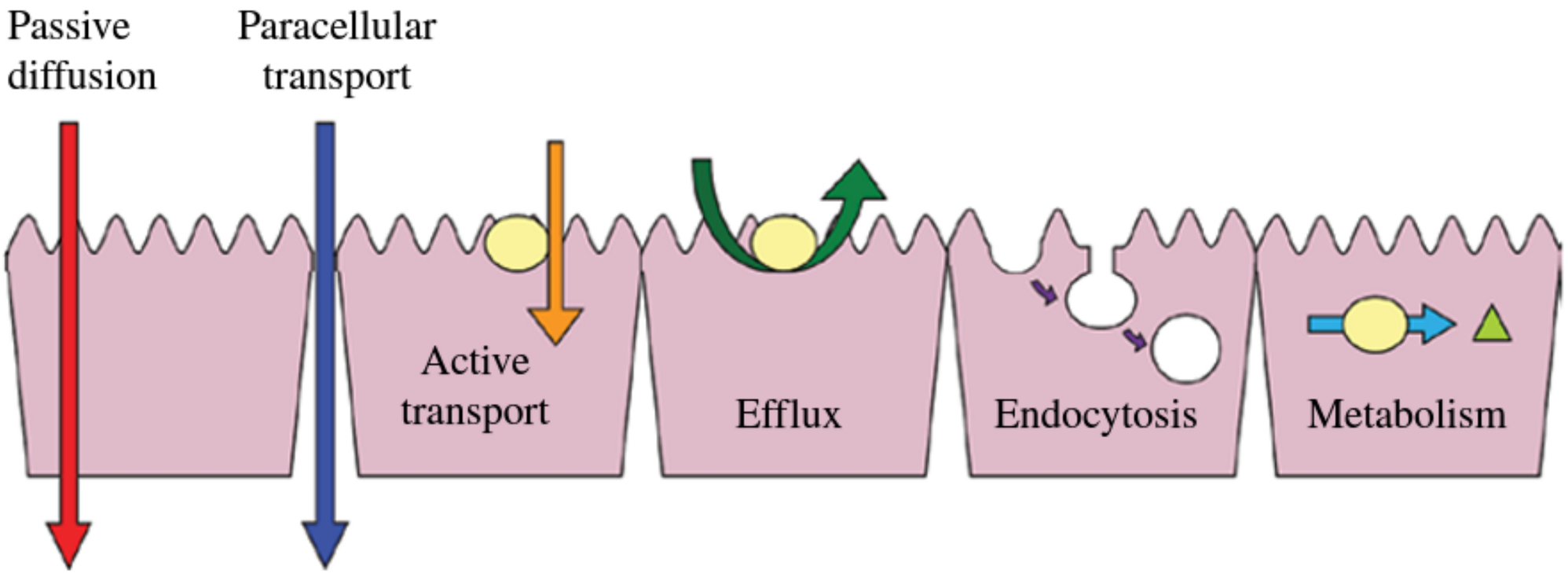

FIGURE 7.3 General mechanisms of drug transport across a cellular barrier. It should be noted that active, facilitative, and efflux transporter proteins may be present in both apical and basolateral membranes. Metabolizing enzymes within cells may in effect limit the transport of drugs by means of biotransformation to metabolites with altered or no pharmacological activity.

can be screened at an earlier stage of development. The reason that a cell culture model is a valid way to assess drug permeability is because the intestinal epithelium is the limiting barrier for the permeation and absorption of drugs [17].

The intestinal mucosa comprises a monolayer of many different cell types. These cells include enterocytes, goblet cells, lymphocytes, M cells, and crypt cells; each cell type has a unique function. Of these cells, enterocytes are the most numerous and form the basis of most cell culture models [18]. Enterocytes are coated with microvilli on the apical surface, which allows for greater surface area and, thus, a higher ability to interact with the luminal contents of the bowel.

The determinants of absorption of drugs through the intestinal epithelium are the permeability of the drug, solubility, and stability. The apparent permeability (P_e) quantifies the rate at which molecules can cross the epithelium [19]. (Readers are referred to previous examples in the literature that demonstrate the calculation of permeability from drug transport experiments [12, 15].) There are many mechanisms by which drugs can permeate through the intestinal epithelium (see Fig. 7.3). The paracellular pathway involves passage through tight junctions that exist between cells, namely, occludins and claudins [20]. Molecules can also cross transcellularly by passive diffusion through the lipid membrane. This pathway of absorption is characteristic of lipophilic molecules [21]. The transcellular pathway includes active and facilitated transport, both of which use specific proteins in the cell membranes to allow passage of molecules into and through the cell. A number of influx and efflux transporters (e.g., P-glycoprotein) exist in the membrane that also regulate the passage of certain substrates.

7.3.2 Intestinal Epithelial Cell Culture Models

To date, a number of *in vitro* models of the intestinal epithelium have been investigated, all of which may possess different characteristics and, thus, have different potential applications in the study of drug transport. A number of reviews have been

published comparing the usefulness of these models in ranking the order of drug permeability as well as correlations to the *in vivo* situation.

Primary cell culture techniques for the intestinal epithelium have been developed. However, these models typically cannot form monolayers and are not polarized. Immortalized cell lines have the advantage of forming monolayers and expressing a phenotype similar to the mature intestinal epithelium. The most widely used model is the Caco-2 cell line. This cell line originated from adenocarcinoma of the colon, but it resembles the small intestine in terms of transporter expression. Once this cell line reaches confluence in culture, it spontaneously changes the phenotype to mature epithelium [17]. The expression of transporters in this model is actually less than found *in vivo* [19]. Because of these factors, its usefulness is limited to studying the transport of drugs that display high passive transport across the epithelium [20]. The intercellular pore size of Caco-2 cells is 4.5 Å, which is smaller than the normal intestinal pore size of 8–13 Å [22]. Depending on the mechanism of transport, it can be useful for specific transport studies [19]. Many transporters present in the intestinal epithelium are expressed by Caco-2 cells, including MDR1 (P-glycoprotein) and ABCG2 (breast cancer-resistant protein, BCRP). Several metabolic enzymes are also expressed, including CYP1A. CYP3A4 can also be induced in this cell line by administration of vitamin D3 [22]. A disadvantage of this cell line, however, is that it is heterogeneous. It also lacks many characteristics of the *in vivo* intestinal epithelium. To that end, other models involving the Caco-2 system have been developed. For instance, there exists a subclone called TC7, which is useful in that it expresses many brush border enzymes [17].

Other cell lines that can mimic the intestinal epithelium are the Madin-Darby canine kidney epithelial cell line (MDCK) and the 2/4/A1 cell line. MDCK cells are derived from the renal epithelium of dogs and are useful for studying membrane permeability. It is similar to Caco-2 in its predictive power of the behavior of drugs *in vivo*. The 2/4/A1 cell line, however, is derived from the rat small intestine. It has a better predictive capability than the Caco-2 cell line, even though it lacks several transporters. It is useful for soluble compounds and demonstrates passive diffusion characteristics similar to intestinal epithelium *in vivo* [19].

Coculture models, which demonstrate more features of the heterogeneous cell population of the intestinal epithelium, can provide more insight into drug behavior in the intestine. Examples of this include the Caco-2/HT29 model, which produces mucus, and the Caco-2/Raji-B coculture model, which is meant to mimic follicle-associated epithelium. A triple culture of Caco-2/HT29/Raji-B cells has also been developed [17].

7.4 THE BLOOD–BRAIN BARRIER

7.4.1 The Blood–Brain Endothelial Barrier

The blood–brain barrier (BBB) is composed of the brain microvascular endothelial cells (BMECs) and is a part of the neurovascular unit. Perivascular cells (pericytes and astrocytes) contribute to the basement membrane, surrounding the capillaries

and containing structural proteins, collagens, and specialized proteins [23–25]. This barrier functions as an interface between the brain parenchyma and the systemic circulation. The BBB is largely impermeable to the transfer of most compounds; for example, clinical trials have shown that 98% of drugs intended to treat cancers in the central nervous system had inadequate BBB permeability [26–28].

Several features of the brain endothelium contribute to its functional barrier and limit the permeability of many drugs. These include tight interendothelial junctions, which limits paracellular permeability; few pinocytic vesicles and a low level of endocytosis and transcytosis; an enzymatic barrier, which includes acetylcholinesterase, alkaline phosphatase, γ-glutamyl transpeptidase, monoamine oxidases, and drug metabolizing enzymes; and efflux transporters [29]. The tight junctions are characterized with high transendothelial electrical resistance values in the range of 1500–2000 $\Omega\,cm^2$, and selective transporter proteins within the BBB include efflux proteins such as P-glycoprotein (ABCB1, MDR1), BCRP (ABCG2), multidrug resistance associated proteins (MRPs, ABCC1-6), and organic anion transporters (OATs), but carrier-mediated solute carriers and endocytosis mechanisms are also present [26, 27, 29–31].

7.4.2 BBB Cell Culture Models

Since there is a large market for central nervous system drugs to treat or prevent a number of disorders (e.g., epilepsy, multiple sclerosis, Alzheimer's disease, inflammation, edema, hypoxia, ischemia, glaucoma, Parkinson's disease, depression, and HIV), several BBB models—ranging from in silico to *in vivo*—have been developed to predict the pharmacodynamic and pharmacokinetic behavior of many different classes of drugs [25, 26, 32–37]. Primary cell culture models of the BBB are based on the isolation of BMECs from various species. Bovine BMECs (BBMECs) and porcine BMECs (PBMECs) are most commonly used [38]. Primary cells can also be cocultured with astroglial cells, neurons, pericytes, and/or astrocytes in order to approximate *in vivo* conditions more closely [39–42]. Additional modifications to mimic *in vivo* conditions include the use of a plate viscometer or a cone-plate apparatus to build a dynamic model, and materials such as collagen, hydrogels, extracellular matrix proteins, or polypropylene can be used to create a three-dimensional (3D) scaffold or a hollow organ-like structure to improve *in vitro* modeling of the BBB. Contact coculture and 3D dynamic models closely mimic the *in vivo* BBB, and high transendothelial electrical resistance values have been obtained with such models (up to 1650 $\Omega\,cm^2$) [25, 29, 31, 40, 41, 43].

Several immortalized cell line models of the BBB have been developed, including cell lines of human origin (HMEC-1, hCMEC/D3, and TY08), rat origin (RBE4, GP8, GPNT, and TR-BBB), and murine origin (bEnd.3-5 and TM-BBB) [25, 29, 31, 40, 42, 44, 45]. Readers are referred to recently published examples of culturing protocols for the hCMEC/D3 and bEnd.5 cell lines [23]. As was the case for primary cell culture models, the addition of astrocytes, pericytes, neurons, and glial cells can improve barrier function (increases in transendothelial electrical resistance values, expression of transporters, induction of relevant enzymes, and decreases in passive and paracellular permeability) [29–31, 39–41, 45, 46]. For example, coculture of

hCMEC/D3 cells with astrocytes resulted in significant increases in transendothelial electrical resistance values. However, exposing the cells to flow-based shear stress resulted in the most substantial increases in transendothelial electrical resistance, with values exceeding 1000 $\Omega\,cm^2$ [31]. The development of human pluripotent stem cell–derived BMECs has been described recently, which may be useful in future drug screening applications [40].

7.5 NASAL AND PULMONARY EPITHELIUM

7.5.1 The Respiratory Airway Epithelial Barrier

The pulmonary system is the site of gas exchange between the blood and air. It can be categorized into the upper respiratory tract (including the nasal cavity, pharynx, and larynx) and the lower respiratory tract (including the trachea, primary bronchi, bronchioles, and the alveolar region) [47]. The airway diameter decreases progressively along its length until it ends with the alveolar sacs, the distal, functional respiratory units where gas exchange occurs. Healthy human lungs contain between 300 and 500 million alveoli [48].

The entire respiratory system is lined by a continuous layer of epithelial cells (see Fig. 7.4). This epithelial layer plays a number of vital roles: (i) it forms a physical protective barrier, (ii) it facilitates mucociliary clearance, (iii) it secretes protective substances including antimicrobial agents, (iv) it helps regenerate and repair other pulmonary components, and (v) it plays a role in inflammatory and immune responses [47, 50]. The epithelial cell type changes along the respiratory system to accommodate specific functions, which are morphologically and functionally unique to each region.

The epithelium of the upper respiratory tract is composed of stratified squamous cells, and the nasal cavity is composed of transitional nonciliated epithelial cells. This region has traditionally been considered of low interest for drug delivery because of the small surface area and low vascularity. Within the nasal cavity, however, is the olfactory epithelium, located on the upper part of the nasal cavity, which represents approximately 8% of the total nasal surface area [51]. It is composed of pseudostratified ciliated cells, supporting cells, basal cells, Bowman's glands, and olfactory sensory neurons. These olfactory neurons are unique in that they are directly in contact with the nasal cavity environment, and their axons are in contact with the olfactory bulb in the brain. Therefore, the delivery of drugs to the brain is possible by means of intranasal administration [52].

The respiratory epithelium of the pharynx and the larynx consists of ciliated and nonciliated columnar cells, goblet cells, and basal cells. Most of the luminal surfaces of the nasal mucosa are covered with mucus, produced by goblet cells within the surface of the epithelium. This mucus plays an important role in filtering particles from the inhaled air. It also contains several isoforms of cytochrome P-450 enzymes, which are responsible for metabolizing many drugs. The mucus is constantly cleared toward the nasopharynx by the beating cilia (mucociliary clearance), and then cleared through the digestive tract via the esophagus [53].

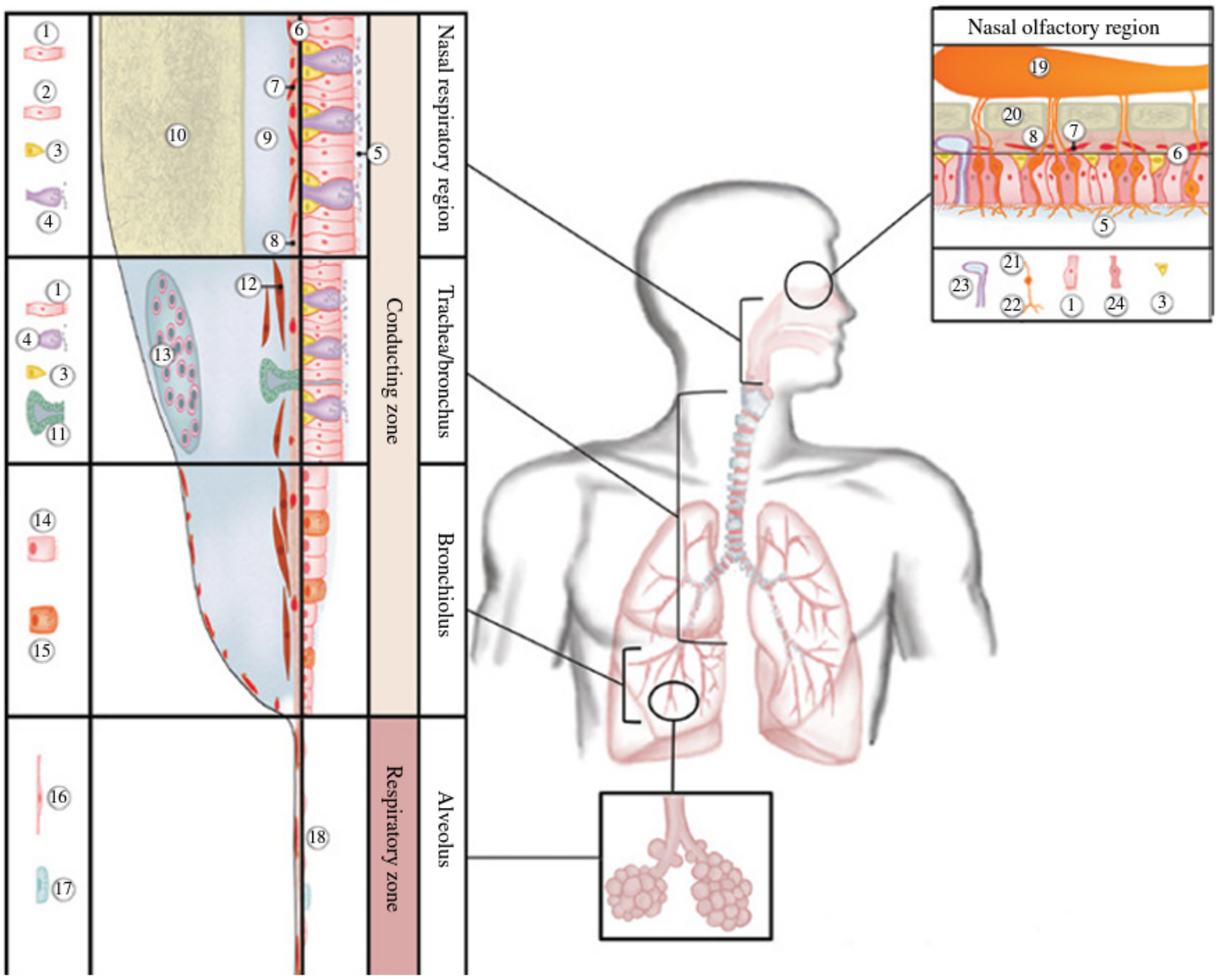

FIGURE 7.4 Cell types lining the respiratory system. Key: (1) ciliated columnar cells, (2) non-ciliated columnar cells, (3) basal cells, (4) goblet cells, (5) mucus, (6) basement membrane, (7) blood vessels, (8) lamina propria, (9) fibro-cartilaginous layer, (10) bone, (11) gland, (12) smooth muscle cells, (13) cartilage, (14) ciliated cuboidal cells, (15) Clara cells, (16) type I alveolar cells, (17) type II alveolar cells, (18) surfactant, (19) olfactory bulb, (20) cribriform plate, (21) receptor cell, (22) receptor cell cilia, (23) Bowman's gland, (24) supporting cell. Adapted from Klein et al. [49], pp. 1516–1534. (*See insert for color representation of the figure*.)

The epithelium in the lower respiratory tract consists of columnar and pseudostratified cells, secretory goblet cells, basal cells, and ciliated cells for mucociliary clearance. In the bronchioles, the epithelium consists of cuboidal cells with short cilia and secretory Clara cells. The distal respiratory tract consists mainly of the alveolar epithelium that is composed of type I and type II alveolar cells. Type II alveolar cells produce surfactant and serve as progenitors for type I alveolar cells [50, 51, 53].

7.5.2 The Nasal Epithelial Barrier and Cell Culture Models

Intranasal drug delivery is noninvasive, results in rapid onset of action, and avoids first-pass metabolism [54]. Several *in vivo* animal models have been evaluated for intranasal delivery; however, these models have failed to correlate well with results

in humans. Therefore, human nasal *in vitro* models have been established as a substitute for such animal models [55].

Primary culture of human nasal epithelial cells provides a promising tool for studying drug transport, metabolism, toxicology, and electrophysiology. These cultures form confluent monolayers in 6–8 days, with differentiated goblet and ciliated cells. The primary human nasal cell can be obtained by several methods. Nevertheless, these methods are limited by intensive labor, limited passage number, heterogeneity, risk of pathogenic contamination, and donor variability. Several factors affect primary nasal epithelial cell culture. For example, prolonged culturing can lead to loss of cilia and supplementary extracellular matrix can affect cell differentiation [56–62].

Some of the limitations of primary culture may be overcome by the use of cell lines. The most common cell line of human origin is RPMI 2650, derived from human nasal anaplastic squamous cell carcinoma of the nasal septum [56, 57]. Nonhuman nasal cell lines include bovine turbinate cells and NAS 2BL (derived from rat nasal squamous carcinoma). Although RPMI 2650 cells may be useful for metabolism studies, they do not form monolayers spontaneously, and they lack goblet and ciliated cells, which makes them unsuitable for drug permeation studies. Nevertheless, it has been reported that the use of RPMI 2650 cells under air–liquid interface culture conditions can promote the formation of a monolayer with sufficient transepithelial electrical resistance (TEER) to perform drug permeation studies [63, 64]. A 3D reconstructed nasal mucosa was recently developed, which also shows promise for drug transport studies [65, 66]. Although Calu-3 cells are not of nasal origin, but are derived from human lung adenocarcinoma, these cells have also been investigated as a screening tool for nasal drug delivery. At an air–liquid interface, Calu-3 cells form a polarized monolayer with suitable TEER values and a uniform mucus layer [61, 64, 67–70]. Additional studies are needed to correlate *in vitro* and *in vivo* results to promote the use of such *in vitro* models in high throughput drug candidate screening.

7.5.3 The Airway Epithelial Barrier and Cell Culture Models

A variety of epithelial cell line models have been developed to specifically study basic cellular pathways, toxicology, and drug transport within the airways. A number of protocols have been developed for culturing primary human airway cells *in vitro* [49, 71, 72]. Primary human cells can be cultured from normal or disease-derived cells. In fact, comparing cultures derived from normal versus diseased cells provides a methodology for probing the underlying pathways that contribute to disease. Primary bronchial epithelial cell monolayers derived from asthmatic donors have been shown to retain their phenotype even after several passages [73]. To better replicate the *in vivo* airway epithelium, complex *in vitro* models have been established, which include coculture techniques and 3D mucus-secreting spheroids of primary bronchial epithelial cells [74–76]. Precultured cell systems are commercially available, such as EpiAirway™ and MucilAir™. The EpiAirway model is prefilled with primary cells of human tracheal or bronchial epithelium, and the MucilAir

model contains primary cells of the human respiratory tract. In both models, the cells are well differentiated, form beating cilia, secrete mucus, and form tight junctions. In addition, they have a long life span and are suitable for uptake and transport studies [17, 48, 49].

Three immortalized cell lines most widely used for investigations of the airway epithelium include Calu-3, 16HBE14o-, and BEAS-2B cells [77]. The Calu-3 adenocarcinoma cell line generates a confluent monolayer with tight junctions and mucus production. Transport studies can be performed after 6–8 days in submerged culture and after 10–14 days in air–interface culture. 16HBE14o- is an immortalized epithelial cell line derived from healthy human bronchial epithelium. The cells form tight junctions, retain differentiated epithelia with apical microvilli, and have no mucus secretion. The 16HBE14o- cell line has been used to study oxidative stress and inflammation, and transport studies can be performed after 6–9 days in submerged culture or after 6–7 days using air–interface culture. Both Calu-3 and 16HBE14o- cells express P-glycoprotein. Like 16HBE14o- cells, BEAS-2B cells are viral transformed human bronchial epithelial cells. However, BEAS-2B cells do not form tight junctions [49, 78–80].

7.5.4 The Alveolar Epithelial Barrier and Cell Culture Models

There are two types of alveolar epithelial cells: type I and type II. Type I alveolar epithelial cells are squamous cells which form the air–blood barrier. These cells cover 95% of the alveolar surface. Type II alveolar epithelial cells are cuboidal, produce surfactant and proinflammatory mediators, and are the progenitors of type I alveolar cells. A population of alveolar macrophages is also found in the interstitial spaces; these macrophages clear pathogens and debris deposited in the air spaces [47, 48, 81, 82].

Primary human alveolar epithelial cells (hAEpC) are derived from type II alveolar cells isolated from human lung biopsies. After 8–9 days in culture, tight junctions are formed and most of the cells are flattened, displaying a type I alveolar cell-like phenotype. To more closely resemble the air–blood barrier, cocultures of hAEpC cells with macrophages, dendritic cells, and/or primary human pulmonary microvascular endothelial cells are possible [83–88]. An innovative alveolar "lung-on-a-chip" model has been described, which provides structural, functional, and mechanical properties of the human alveolar–capillary interface (see Fig. 7.5). The alveolar cells are separated from the endothelial cells by a flexible membrane coated with fibronectin. Nutrients are supplied through microfluidic flow of medium and immune cells, and the flexible membrane allows for the cyclical stretching of alveolar tissue during respiration [87, 88].

The A549 alveolar epithelial cell line derived from a human adenocarcinoma exhibits properties consistent with type II alveolar cells, such as the presence of lamellar bodies and surfactant proteins [89]. However, A549 cells do not differentiate to a type I alveolar cell-like phenotype, and they do not form tight junctions, which limits the use of this cell line for transport studies [90]. NCI-H441 cells are of human distal lung epithelial origin and are more suitable for transport studies. NCI-H441

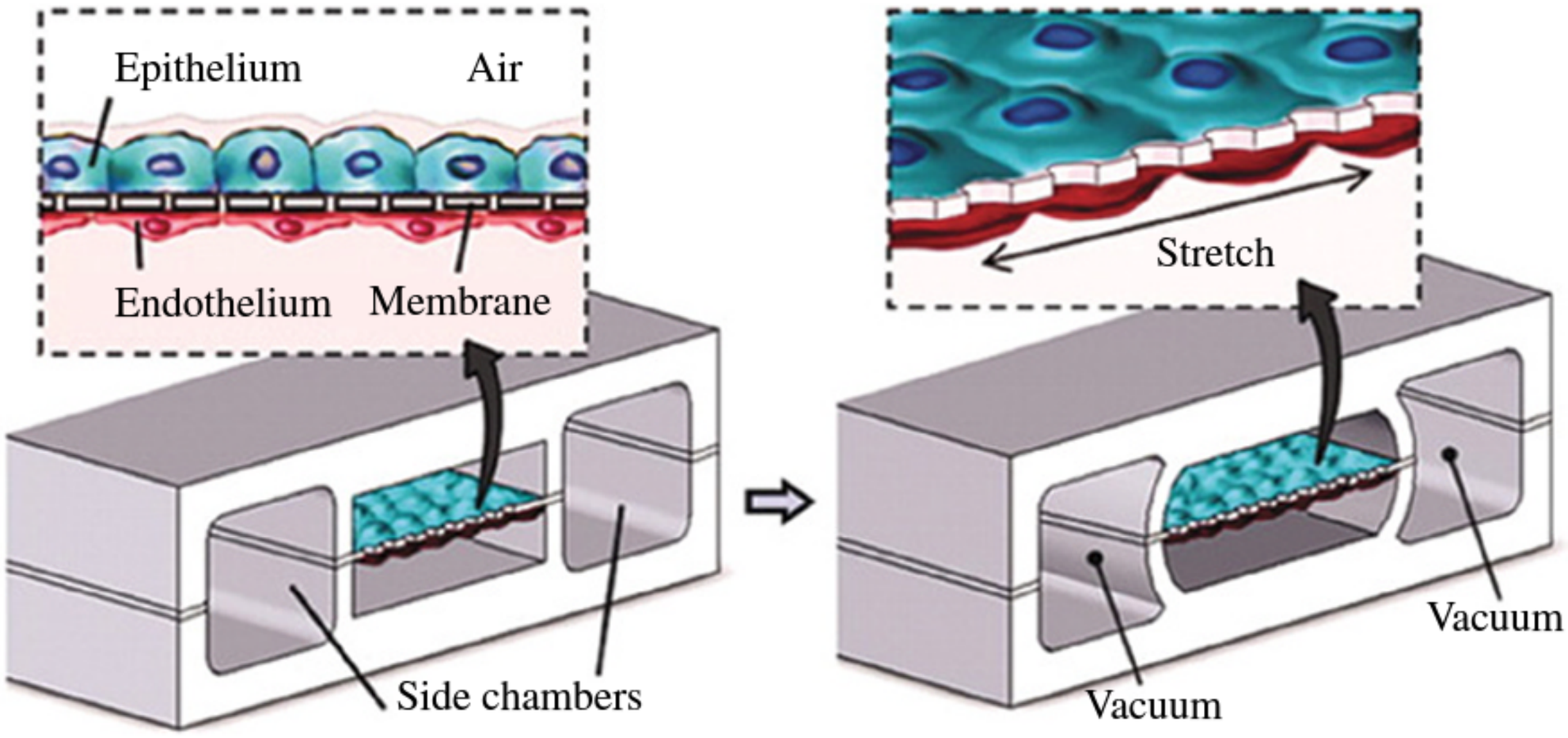

FIGURE 7.5 *In vitro* model of the alveolar–capillary barrier. Cells representing the airway epithelium and pulmonary endothelium are grown on opposite sides of a flexible membrane. Vacuum is applied to the side chambers to mimic physiological breathing, causing mechanical stretching of the flexible membrane. Huh et al. [87], pp. 1662–1668. Reprinted with permission of the AAAS.

cells are derived from human lung papillary adenocarcinoma and in some aspects are representative of the bronchiolar pulmonary epithelium and type II alveolar epithelial cells. In culture, this cell line forms confluent monolayers with tight junctions, with peak TEER values around $1000\,\Omega\,cm^2$. Drug transporter activity and expression is similar to that seen in primary alveolar epithelial cells, including the presence of P-glycoprotein and a number of organic cation transporters [89].

7.6 THE OCULAR EPITHELIAL AND ENDOTHELIAL BARRIERS

7.6.1 The Corneal and Retinal Barriers

The cornea and the conjunctiva are the two major components of the anterior barrier of the eye. The cornea is a clear, avascular layer of epithelial cells that is only 520 μm thick. This layer includes superficial cells, wing cells, basal cells, Bowman's layer, stroma, Descemet's membrane, and endothelium. The tight junctions of the corneal epithelium prevent the paracellular passage of hydrophilic molecules, but passive diffusion is possible for lipophilic compounds. The pores in the intercellular spaces are negatively charged at physiological pH due to the carboxylic groups on the tight junction proteins. The conjunctival layer comprises mucus-producing epithelial cells. It acts as a protective surface that maintains the tear film by production of mucus glycoproteins. The conjunctiva is more permeable to hydrophilic compounds and macromolecules than the cornea. Nevertheless, drug delivery across the conjunctiva is considered nonproductive absorption because most of the drug is lost to the blood rather than reaching a site of action within the aqueous humor [91–94].

The blood–retinal barrier (BRB) consists of outer and inner layers. The retinal pigment epithelial cells form the outer layer, and the retinal vascular endothelial cells form the inner layer. The BRB resembles the BBB in that it limits the transport of molecules between the neural retina and the systemic circulation. Pericytes are important in regulating the permeability of the BRB, and the absence of pericytes can cause vascular leakage. The inner BRB is essential for intact vision and is involved in the transport of nutrients to the retina and the excretion of waste products. Occludin, claudin, and junctional adhesion molecules maintain tight junctions between the retinal vascular endothelial cells. The polarized retinal pigment epithelium separates the neural retina from the choroid and also has tight junctions [95–98].

7.6.2 Cell Culture Models of Ocular Epithelium and Endothelium

Primary cell culture models of the corneal epithelium derived from rabbits have been described for use in permeability studies [95]. Primary human corneal epithelial cells (HCEpiC) have been utilized to characterize the expression of monocarboxylate and efflux transporters [99, 100]. Immortalized cell models of the human corneal epithelium that have been utilized for studying transport include HCE cells, tet HPV16-E6/E7 transduced HCE cells, and HCLE cells [95, 101]. Primary models of the conjunctival epithelium include cells isolated from rabbits, which have shown TEER values similar to that of excised rabbit conjunctiva [95]. An immortalized human conjunctival epithelial cell line (HCjE) has been used to investigate drug transporter expression [101].

Primary cell culture models of the retinal pigment epithelium include cells isolated from both human and animal sources, but to avoid the challenges associated with interspecies data extrapolation, the use of human primary cells is preferred. The human immortalized ARPE-19 cell line has been used extensively to characterize drug transport across the retinal pigment epithelium [95]. A primary bovine cell model of the retinal capillary endothelium can be difficult to grow as a tight monolayer. Human primary retinal endothelial cells (hREC) can also be isolated and have been utilized in permeability studies to assess monolayer integrity [102]. An immortalized cell line of the retinal capillary endothelium (TR-iBRB) was derived from a transgenic rat, but the cells do not form a tight barrier [95]. A telomerase-immortalized cell line (HREC-hTERT) has been derived from human primary cells and may serve as an appropriate model of the human BRB [103].

7.7 THE PLACENTAL BARRIER

7.7.1 The Syncytiotrophoblast Barrier

The placenta is the interface between the mother and the fetus during pregnancy. It serves many functions, such as gas and nutrient exchange, waste elimination, and the metabolism of some drugs. For instance, the oxygen diffusing capacity of the placenta influences gas exchange between the fetal and maternal circulations. The human

syncytiotrophoblast cell layer is replenished by precursor cytotrophoblast cells and has the dual functionality of a transport barrier and a hormone producer [104, 105]. It is the rate-limiting barrier for exchange between the fetal and the maternal circulations, and it is responsible for the regulation of the transport of toxins, xenobiotics, waste products, and nutrients [106]. The mechanism of transport across the placenta varies depending on the size of the molecule. In general, many molecules having molecular weights less than 1000 Da can freely cross the placental barrier by passive diffusion. Other transplacental transport processes exist, namely, facilitated diffusion (not requiring metabolic energy) and active transport (requiring metabolic energy) [107]. Syncytiotrophoblast cells are polarized, with basolateral (facing the fetus) and apical (facing the mother) plasma membranes. The polarity of the syncytiotrophoblast layer has an important role in regulating the movement of nutrients and waste products between the maternal and fetal circulations [105, 106]. Transporters in the maternal side include P-glycoprotein (MDR1), BCRP, MRP2, OCTN2, SERT, and NET, while transporters expressed on the fetal side include MRP1, MRP3, MRP5, OATP-B, OAT4, OCT3, and MDR3 [108].

7.7.2 Trophoblast Cell Culture Models

In vitro models to elucidate drug transport and uptake in placental trophoblast cells include isolated tissue explants, primary cells, and immortalized cell lines. The use of placental tissue explants, membrane vesicles, and primary cytotrophoblast cells can provide information regarding placental drug uptake, but these systems do not form confluent monolayers sufficient to carry out transport studies [14, 109]. Immortalized trophoblast cell culture models include JEG-3 cells, JAr cells, and BeWo cells. JEG-3 and JAr cells secrete placental hormones can syncytialize in culture and can be used for drug uptake studies. However, they are generally considered unsuitable for polarized transport experiments [110]. It should be noted that two clones of the BeWo cell line (b24 and b30) form confluent monolayers amenable to drug transport studies, but the original BeWo cell line available through the American Type Culture Collection does not have this same monolayer-forming ability [12, 14]. BeWo b30 cells have been utilized in a number of drug transport and metabolism studies [111, 112]. In fact, recent comparisons have demonstrated very good correlation between *in vitro* permeability data from BeWo b30 cell transport experiments and measurements of drug transfer across *ex vivo* dually perfused human placental lobules [12, 113].

7.8 THE RENAL EPITHELIUM

7.8.1 The Renal Epithelial Barrier

The kidneys are highly perfused; blood flow to the kidneys is approximately 25% of total cardiac output. Each kidney contains more than 1 million nephrons. Within a single nephron, blood undergoes glomerular filtration. Most substances having a

molecular weight below 5000 Da pass through the glomerulus, whereas most proteins remain in the capillaries. The plasma ultrafiltrate moves from the glomerulus into the proximal tubule, Henle's loop, the distal tubule, and finally as urine into the collecting duct. Tubular secretion and reabsorption processes take place along this pathway to maintain fluid and electrolyte balance and concentrate the urine. A number of nutrients and ions are reabsorbed from the filtrate into the blood. Osmotic pressure promotes the reabsorption of water from the filtrate back into the renal capillaries. The renal tubules are lined with epithelial cells, which contain a number of transporter proteins that participate in tubular secretion mechanisms. The apical (brush border) membrane faces the urine, and basolateral infoldings of the epithelium interact with the renal capillaries. Certain drugs (ionized compounds in particular) may be actively secreted against a concentration gradient out of the blood and into the filtrate, whereas other drugs (e.g., unionized lipophilic compounds) may diffuse across the tubular epithelium and be reabsorbed into the blood. [114, 115].

7.8.2 Renal Epithelial Cell Culture Models

A number of cell culture models have been described for studying tubular secretion and reabsorption. This paragraph will introduce primary cell models, and the following paragraph will discuss some of the advantages and limitations of certain cell line models. Terryn et al. have isolated primary proximal tubule cells from mice [116]. Markadieu et al. have described a unique method to isolate primary cultured distal tubule cells from mice expressing enhanced green fluorescent protein under the parvalbumin promoter. Parvalbumin is expressed in the distal convoluted tubule. Fluorescent parvalbumin–containing tubules were separated and a cellular monolayer with tight junctions was established [117]. Primary proximal tubular cells from porcine kidney were confirmed to express several important transporters, although some transporters that were expressed in freshly isolated cells were down-regulated in culture [118]. Taub has reported the use of hormonally defined serum-free media to promote the differentiation of primary rabbit kidney tubule epithelial cells without fibroblast overgrowth. The resulting cells had a polarized morphology and tight junctions [119]. A similar approach was applied to the isolation of primary human proximal tubule cells by a Percoll gradient, followed by culture in hormonally defined serum-free media, which allowed the formation of a tight monolayer for up to three passages [120]. Another technique for separating primary human proximal tubule cells involves the use of antibodies to CD10 and CD13 as markers of proximal tubule epithelial cells in conjunction with fluorescence activating cell sorting (FACS) [121]. Primary cultured human proximal tubule cells express a number of transporters relevant to drug disposition, and they can be cultured on Millicell® filter inserts or on Transwell inserts [122]. Jang et al. cultured primary human proximal tubule cells on a microfluidic device whereon the monolayer is exposed to fluid shear stress. This resulted in enhanced cell polarization and formation of cilia compared to the growth of cells on Transwell inserts [123].

Cell lines as models for renal tubular epithelial cells include: MDCK cells (canine); OK cells (opossum); LLC-PK_1 (porcine); PKSV-PCT, PKSV-PR, and

mpkCCD$_{cl4}$ (murine); and HKC, HK-2, Caki-1, and RPTEC/TERT1 cells (human). MDCK cells represent the distal renal epithelium and express P-glycoprotein, monocarboxylic acid, organic cation, and peptide transporters, as well as alkaline phosphatase, glutathione S-transferase, and sulfotransferase. When grown on semipermeable inserts, MDCK cells are polarized and form tight junctions. MDCK cells have been used as a model of intestinal drug absorption because, similar to Caco-2 cells, MDCK permeability values correlate with drug absorption, and MDCK cells grow faster than Caco-2 cells [124]. OK opossum kidney cells have been shown to reflect the *in vivo* paracellular permeability properties of rat proximal tubules [125]. In LLC-PK$_1$ proximal tubule cells, apical SGLT and basolateral GLUT are highly expressed, and the cells have a moderate expression of OCTs and OATs [126]. Chassin et al. have described the derivation of the proximal tubule cell lines PKSV-PCT and PKSV-PR from transgenic mice, as well as the mpkCCD$_{cl4}$ collecting duct cell line [127]. HKC-8 cells express the Na^+-HCO_3^- cotransporter (NBC-1) with transport activity similar to that of intact proximal tubules [128]. HK-2 cells express SLC16A1 (MCT) and SLCO4C1 (OATP4C1), MDR1, and MRPs, but they do not express the SLC22 transporters OAT1, OAT3, and OCT2, nor do they express ABCG2 (BCRP) [129]. The TEER of Caki-1 cells was stable between passage numbers 8 and 71 and was representative of a leaky epithelium. Although they retain activity of certain transport proteins and metabolizing enzymes, in comparison to native kidney cells, Caki-1 cells have high expression of MRP3, MRP4, and MRP6, and low levels of MDR1 [129, 130]. RPTEC/TERT1 cells display intact vectorial transport and hormonal response similar to primary cells, but this cell line is genomically stable for up to 90 population doublings [131].

7.9 3D *IN VITRO* MODELS

Because two-dimensional cell monolayers cannot fully represent the 3D nature and extracellular matrices of tissues *in vivo*, the development of 3D *in vitro* models can provide a cellular microenvironment that preserves cell–cell interactions and tissue architecture. 3D cellular models can provide environmental cues affecting cell signaling, differentiation, and morphology [132–134]. A number of cellular 3D models have been developed, including models of liver, breast, cardiac, muscle, bone, corneal tissue, and tumors. 3D tumor models include multicellular spheroids, hollow fibers, and multicellular layers. Spheroids, for example, mimic the heterogeneity of tumor cells, having a hypoxic, necrotic region in the core [133].

3D tissue constructs can be developed by top-down or bottom-up approaches. In a top-down approach, cells are seeded in a biodegradable scaffold, but it can be difficult to control cell alignment or cell–cell interactions by this method. Four types of bottom-up approaches include cellular layer-by-layer, extracellular matrix-assisted cellular layer-by-layer, cell accumulation, and inkjet printing of cells and polymers. One cellular layer-by-layer approach utilizes temperature-sensitive polymeric culture dishes to harvest a layer of cells without using proteolytic enzymes. Cell sheets can then be stacked to create the 3D model. In the extracellular matrix-assisted layer-by-layer

technique, a film of fibronectin and gelatin is placed on cell monolayers, onto which a second cell seeding can be performed. This process can be repeated to generate the desired 3D cellular structure. The cell accumulation method involves coating single cells with fibronectin and gelatin, which promotes cell–cell adhesion [134]. In one example of a 3D model, Astashkina et al. used a hyaluronic acid hydrogel to encapsulate an intact proximal tubule, that is, not just the epithelial cells. These 3D organoid proximal tubule cultures were more sensitive to toxic insult than 2D LLC-PK_1 or HEK293 cells [132, 135].

7.10 CONCLUSIONS

The application of cell culture models for predicting drug transport has facilitated an accelerated pace of understanding the biochemical processes affecting the permeability of molecules across cellular barriers. Besides serving as a tool for screening passive permeability and studying uptake and efflux mechanisms, many of these same cell lines also play a number of roles in various pharmacological and toxicological assays. It is interesting to review the previous edition of this chapter, which contained expressions of hope for future developments, including a more convenient model of the BBB and 3D cellular models. As we appreciate and welcome these advances, which have been realized during the past decade, we look forward to future refinements and opportunities to improve our understanding of drug transport and improve our clinical approaches to drug delivery.

REFERENCES

1. Audus, K. L.; Bartel, R. L.; Hidalgo, I. J.; Borchardt, R. T. *Pharm Res* 1990, **7**, 435–451.
2. Gotz, C.; Pfeiffer, R.; Tigges, J.; Blatz, V.; Jackh, C.; Freytag, E. M.; Fabian, E.; Landsiedel, R.; Merk, H. F.; Krutmann, J.; Edwards, R. J.; Pease, C.; Goebel, C.; Hewitt, N.; Fritsche, E. *Exp Dermatol* 2012, **21**, 358–363.
3. Suhonen, M. T.; Pasonen-Seppanen, S.; Kirjavainen, M.; Tammi, M.; Tammi, R.; Urtti, A. *Eur J Pharm Sci* 2003, **20**, 107–113.
4. Sahi, J.; Grepper, S.; Smith, C. *Curr Drug Discov Technol* 2010, **7**, 188–198.
5. Swift, B.; Pfeifer, N. D.; Brouwer, K. L. *Drug Metab Rev* 2010, **42**, 446–471.
6. Malinen, M. M.; Palokangas, H.; Yliperttula, M.; Urtti, A. *Tissue Eng Part A* 2012, **18**, 2418–2425.
7. Forrest, I. A.; Murphy, D. M.; Ward, C.; Jones, D.; Johnson, G. E.; Archer, L.; Gould, F. K.; Cawston, T. E.; Lordan, J. L.; Corris, P. A. *Eur Respir J* 2005, **26**, 1080–1085.
8. Petroff, M. G.; Phillips, T. A.; Ka, H.; Pace, J. L.; Hunt, J. S. *Methods Mol Med* 2006, **121**, 203–217.
9. Freshney, R. I. Basic Principles of Cell Culture. In *Culture of Cells for Tissue Engineering*; Vunjak-Novakovic, G., Freshney, R. I., Eds.; John Wiley & Sons, Inc.: Hoboken, NJ, 2006, 3–22.

10. Soule, H. D.; Maloney, T. M.; Wolman, S. R.; Peterson, W. D., Jr.; Brenz, R.; McGrath, C. M.; Russo, J.; Pauley, R. J.; Jones, R. F.; Brooks, S. C. *Cancer Res* 1990, **50**, 6075–6086.
11. Serrano, M. A.; Macias, R. I.; Briz, O.; Monte, M. J.; Blazquez, A. G.; Williamson, C.; Kubitz, R.; Marin, J. J. *Placenta* 2007, **28**, 107–117.
12. Poulsen, M. S.; Rytting, E.; Mose, T.; Knudsen, L. E. *Toxicol In Vitro* 2009, **23**, 1380–1386.
13. Gumbleton, M.; Audus, K. L. *J Pharm Sci* 2001, **90**, 1681–1698.
14. Bode, C. J.; Jin, H.; Rytting, E.; Silverstein, P. S.; Young, A. M.; Audus, K. L. *Methods Mol Med* 2006, **122**, 225–239.
15. Tavelin, S.; Grasjo, J.; Taipalensuu, J.; Ocklind, G.; Artursson, P. *Methods Mol Biol* 2002, **188**, 233–272.
16. Ho, N. F. H.; Raub, T. J.; Burton, P. S.; Barsuhn, C. L.; Adson, A.; Audus, K. L.; Borchardt, R. T. Quantitative Approaches to Delineate Passive Transport Mechanisms in Cell Culture Monolayers. In *Transport Processes in Pharmaceutical Systems*; Amidon, G. L., Lee, P. I., Topp, E. M., Eds.; Marcel Dekker: New York, 2000, 219–316.
17. Sarmento, B.; Andrade, F.; da Silva, S. B.; Rodrigues, F.; das, N. J.; Ferreira, D. *Expert Opin Drug Metab Toxicol* 2012, **8**, 607–621.
18. Hidalgo, I. J. *Curr Top Med Chem* 2001, **1**, 385–401.
19. Fagerholm, U. *J Pharm Pharmacol* 2007, **59**, 905–916.
20. Baumgart, D. C.; Dignass, A. U. *Curr Opin Clin Nutr Metab Care* 2002, **5**, 685–694.
21. Volpe, D. A. *Future Med Chem* 2011, **3**, 2063–2077.
22. Sun, H.; Chow, E. C.; Liu, S.; Du, Y.; Pang, K. S. *Expert Opin Drug Metab Toxicol* 2008, **4**, 395–411.
23. Czupalla, C. J.; Liebner, S.; Devraj, K. *Methods Mol Biol* 2014, **1135**, 415–437.
24. Vandenhaute, E.; Dehouck, L.; Boucau, M. C.; Sevin, E.; Uzbekov, R.; Tardivel, M.; Gosselet, F.; Fenart, L.; Cecchelli, R.; Dehouck, M. P. *Curr Neurovasc Res* 2011, **8**, 258–269.
25. Naik, P.; Cucullo, L. *J Pharm Sci* 2012, **101**, 1337–1354.
26. Geldenhuys, W. J.; Allen, D. D.; Bloomquist, J. R. *Expert Opin Drug Metab Toxicol* 2012, **8**, 647–653.
27. Adkins, C. E.; Mittapalli, R. K.; Manda, V. K.; Nounou, M. I.; Mohammad, A. S.; Terrell, T. B.; Bohn, K. A.; Yasemin, C.; Grothe, T. R.; Lockman, J. A.; Lockman, P. R. *Front Pharmacol* 2013, **4**, 136.
28. Pardridge, W. M. *Drug Discov Today* 2007, **12**, 54–61.
29. Wilhelm, I.; Fazakas, C.; Krizbai, I. A. *Acta Neurobiol Exp* 2011, **71**, 113–128.
30. Kusuhara, H.; Sugiyama, Y. *NeuroRx* 2005, **2**, 73–85.
31. Weksler, B.; Romero, I. A.; Couraud, P. O. *Fluids Barriers CNS* 2013, **10**, 16–10.
32. Zlokovic, B. V. *Neuron* 2008, **57**, 178–201.
33. Kaur, C.; Ling, E. A. *Curr Neurovasc Res* 2008, **5**, 71–81.
34. Desai, B. S.; Monahan, A. J.; Carvey, P. M.; Hendey, B. *Cell Transplant* 2007, **16**, 285–299.
35. Eugenin, E. A.; Clements, J. E.; Zink, M. C.; Berman, J. W. *J Neurosci* 2011, **31**, 9456–9465.

36. Marchi, N.; Granata, T.; Ghosh, C.; Janigro, D. *Epilepsia* 2012, **53**, 1877–1886.
37. Grieshaber, M. C.; Flammer, J. *Surv Ophthalmol* 2007, **52** Suppl 2, S115–S121.
38. Kuhnline Sloan, C. D.; Nandi, P.; Linz, T. H.; Aldrich, J. V.; Audus, K. L.; Lunte, S. M. *Annu Rev Anal Chem (Palo Alto Calif)* 2012, **5**, 505–531.
39. Fletcher, N. F.; Callanan, J. J. Cell Culture Models of the Blood–Brain Barrier: New Research. In *The Blood–Brain Barrier: New Research*; Montenegro, P. A., Juarez, S. M., Eds.; Nova Science Publishers: Hauppauge, NY, 2012.
40. Lippmann, E. S.; Al Ahmad, A.; Palecek, S. P.; Shusta, E. V. *Fluids Barriers CNS* 2013, **10**, 2–10.
41. Cohen-Kashi, M. K.; Cooper, I.; Teichberg, V. I. *Brain Res* 2009, **1284**, 12–21.
42. Li, G.; Simon, M. J.; Cancel, L. M.; Shi, Z. D.; Ji, X.; Tarbell, J. M.; Morrison, B., III; Fu, B. M. *Ann Biomed Eng* 2010, **38**, 2499–2511.
43. Lu, J. *J Exp Integr Med* 2012, **2**, 39–43.
44. Sano, Y.; Kashiwamura, Y.; Abe, M.; Dieu, L. H.; Huwyler, J. Ã.; Shimizu, F.; Haruki, H.; Maeda, T.; Saito, K.; Tasaki, A. *Clin Exp Neuroimmunol* 2013, **4**, 92–103.
45. Vernon, H.; Clark, K.; Bressler, J. P. *Methods Mol Biol* 2011, **758**, 153–168.
46. Terasaki, T.; Ohtsuki, S.; Hori, S.; Takanaga, H.; Nakashima, E.; Hosoya, K. *Drug Discov Today* 2003, **8**, 944–954.
47. Chang, M. M.-J.; Shih, L.; Wu, R. Pulmonary Epithelium: Cell Types and Functions. In *The Pulmonary Epithelium in Health and Disease*; Proud, D., Ed.; John Wiley & Sons, Ltd: Chichester, 2008.
48. Berube, K.; Prytherch, Z.; Job, C.; Hughes, T. *Toxicology* 2010, **278**, 311–318.
49. Klein, S. G.; Hennen, J.; Serchi, T.; Blomeke, B.; Gutleb, A. C. *Toxicol In Vitro* 2011, **25**, 1516–1534.
50. Toppila-Salmi, S.; Renkonen, J.; Joenvaara, S.; Mattila, P.; Renkonen, R. *Curr Opin Allergy Clin Immunol* 2011, **11**, 29–32.
51. Ali, J.; Ali, M.; Baboota, S.; Sahani, J. K.; Ramassamy, C.; Dao, L.; Bhavna. *Curr Pharm Des* 2010, **16**, 1644–1653.
52. Ugwoke, M. I.; Agu, R. U.; Verbeke, N.; Kinget, R. *Adv Drug Deliv Rev* 2005, **57**, 1640–1665.
53. Harkema, J. R.; Carey, S. A.; Wagner, J. G. *Toxicol Pathol* 2006, **34**, 252–269.
54. Pires, A.; Fortuna, A.; Alves, G.; Falcao, A. *J Pharm Pharm Sci* 2009, **12**, 288–311.
55. Werner, U.; Kissel, T. *Pharm Res* 1996, **13**, 978–988.
56. Merkle, H. P.; Ditzinger, G.; Lang, S. R.; Peter, H.; Schmidt, M. C. *Adv Drug Deliv Rev* 1998, **29**, 51–79.
57. Yoon, J. H.; Kim, K. S.; Kim, S. S.; Lee, J. G.; Park, I. Y. *Ann Otol Rhinol Laryngol* 2000, **109**, 594–601.
58. Yoo, J. W.; Kim, Y. S.; Lee, S. H.; Lee, M. K.; Roh, H. J.; Jhun, B. H.; Lee, C. H.; Kim, D. D. *Pharm Res* 2003, **20**, 1690–1696.
59. Cho, H. J.; Termsarasab, U.; Kim, J. S.; Kim, D. D. *J Pharm Invest* 2010, **40**, 321–332.
60. Gray, T.; Koo, J. S.; Nettesheim, P. *Toxicology* 2001, **160**, 35–46.
61. Cho, H. J.; Balakrishnan, P.; Shim, W. S.; Chung, S. J.; Shim, C. K.; Kim, D. D. *Int J Pharm* 2010, **400**, 59–65.

62. Lee, M. K.; Yoo, J. W.; Lin, H.; Kim, Y. S.; Kim, D. D.; Choi, Y. M.; Park, S. K.; Lee, C. H.; Roh, H. J. *Drug Deliv* 2005, **12**, 305–311.
63. Bai, S.; Yang, T.; Abbruscato, T. J.; Ahsan, F. *J Pharm Sci* 2008, **97**, 1165–1178.
64. Harikarnpakdee, S.; Lipipun, V.; Sutanthavibul, N.; Ritthidej, G. C. *AAPS PharmSciTech* 2006, **7**, E12.
65. Wengst, A.; Reichl, S. *Eur J Pharm Biopharm* 2010, **74**, 290–297.
66. Reichl, S.; Becker, K. *J Pharm Pharmacol* 2012, **64**, 1621–1630.
67. Foster, K. A.; Avery, M. L.; Yazdanian, M.; Audus, K. L. *Int J Pharm* 2000, **208**, 1–11.
68. Berger, J. T.; Voynow, J. A.; Peters, K. W.; Rose, M. C. *Am J Respir Cell Mol Biol* 1999, **20**, 500–510.
69. Teijeiro-Osorio, D.; Remunan-Lopez, C.; Alonso, M. J. *Biomacromolecules* 2009, **10**, 243–249.
70. Amoako-Tuffour, M.; Yeung, P. K.; Agu, R. U. *Acta Pharm* 2009, **59**, 395–405.
71. Wicks, J.; Haitchi, H. M.; Holgate, S. T.; Davies, D. E.; Powell, R. M. *Thorax* 2006, **61**, 313–319.
72. Larsen, K.; Malmstrom, J.; Wildt, M.; Dahlqvist, C.; Hansson, L.; Marko-Varga, G.; Bjermer, L.; Scheja, A.; Westergren-Thorsson, G. *Respir Res* 2006, **7**, 11.
73. Bucchieri, F.; Puddicombe, S. M.; Lordan, J. L.; Richter, A.; Buchanan, D.; Wilson, S. J.; Ward, J.; Zummo, G.; Howarth, P. H.; Djukanovic, R.; Holgate, S. T.; Davies, D. E. *Am J Respir Cell Mol Biol* 2002, **27**, 179–185.
74. Deslee, G.; Dury, S.; Perotin, J. M.; Al Alam, D.; Vitry, F.; Boxio, R.; Gangloff, S. C.; Guenounou, M.; Lebargy, F.; Belaaouaj, A. *Respir Res* 2007, **8**, 86.
75. Wu, X.; Peters-Hall, J. R.; Bose, S.; Pena, M. T.; Rose, M. C. *Am J Respir Cell Mol Biol* 2011, **44**, 914–921.
76. Kunz-Schughart, L. A.; Freyer, J. P.; Hofstaedter, F.; Ebner, R. *J Biomol Screen* 2004, **9**, 273–285.
77. Forbes, I. I. *Pharm Sci Technol Today* 2000, **3**, 18–27.
78. Atsuta, J.; Sterbinsky, S. A.; Plitt, J.; Schwiebert, L. M.; Bochner, B. S.; Schleimer, R. P. *Am J Respir Cell Mol Biol* 1997, **17**, 571–582.
79. Manford, F.; Tronde, A.; Jeppsson, A. B.; Patel, N.; Johansson, F.; Forbes, B. *Eur J Pharm Sci* 2005, **26**, 414–420.
80. Forbes, B.; Ehrhardt, C. *Eur J Pharm Biopharm* 2005, **60**, 193–205.
81. Mühlfeld, C.; Ochs, M. Functional Aspects of Lung Structure as Related to Interaction with Particles. In *Particle-Lung Interactions*, 2nd ed.; Gehr, P., Mühlfeld, C., Rothen-Rutishauser, B., Blank, F., Eds.; Informa Healthcare: New York, 2010, 1–16.
82. Möller, W.; Kreyling, W. G.; Schmid, O.; Semmler-Behnke, M.; Schulz, H. Deposition, Retention and Clearance, and Translocation of Inhaled Fine and Nano-Sized Particles. In *Particle-Lung Interactions*, 2nd ed.; Gehr, P., Mühlfeld, C., Rothen-Rutishauser, B., Blank, F., Eds.; Informa Healthcare: New York, 2010, 79–107.
83. Sakagami, M. *Adv Drug Deliv Rev* 2006, **58**, 1030–1060.
84. Lehmann, A. D.; Daum, N.; Bur, M.; Lehr, C. M.; Gehr, P.; Rothen-Rutishauser, B. M. *Eur J Pharm Biopharm* 2011, **77**, 398–406.
85. Alfaro-Moreno, E.; Nawrot, T. S.; Vanaudenaerde, B. M.; Hoylaerts, M. F.; Vanoirbeek, J. A.; Nemery, B.; Hoet, P. H. *Eur Respir J* 2008, **32**, 1184–1194.

86. Hermanns, M. I.; Unger, R. E.; Kehe, K.; Peters, K.; Kirkpatrick, C. J. *Lab Invest* 2004, **84**, 736–752.
87. Huh, D.; Matthews, B. D.; Mammoto, A.; Montoya-Zavala, M.; Hsin, H. Y.; Ingber, D. E. *Science* 2010, **328**, 1662–1668.
88. Choe, M. M.; Tomei, A. A.; Swartz, M. A. *Nat Protoc* 2006, **1**, 357–362.
89. Salomon, J. J.; Muchitsch, V. E.; Gausterer, J. C.; Schwagerus, E.; Huwer, H.; Daum, N.; Lehr, C. M.; Ehrhardt, C. *Mol Pharm* 2014, **11**, 995–1006.
90. Foster, K. A.; Oster, C. G.; Mayer, M. M.; Avery, M. L.; Audus, K. L. *Exp Cell Res* 1998, **243**, 359–366.
91. Kompella, U. B.; Kadam, R. S.; Lee, V. H. *Ther Deliv* 2010, **1**, 435–456.
92. Chang, J. N. *Handbook of Non-Invasive Drug Delivery Systems*, 1st ed.; Elsevier: Burlington, 2010.
93. Holland, E. J.; Mannis, M. J.; Lee, W. B. *Ocular Surface Disease: Cornea, Conjunctiva and Tear Film*; Elsevier Health Sciences: Philadelphia, 2013.
94. Ye, T.; Yuan, K.; Zhang, W.; Song, S.; Chen, F.; Yang, X.; Wang, S.; Bi, J.; Pan, W. *Asian J Pharm Sci* 2013, **8**, 207–217.
95. Hornof, M.; Toropainen, E.; Urtti, A. *Eur J Pharm Biopharm* 2005, **60**, 207–225.
96. Mannermaa, E.; Vellonen, K. S.; Urtti, A. *Adv Drug Deliv Rev* 2006, **58**, 1136–1163.
97. Hosoya, K.; Tachikawa, M. *Adv Exp Med Biol* 2012, **763**, 85–104.
98. Wisniewska-Kruk, J.; Hoeben, K. A.; Vogels, I. M.; Gaillard, P. J.; Van Noorden, C. J.; Schlingemann, R. O.; Klaassen, I. *Exp Eye Res* 2012, **96**, 181–190.
99. Vellonen, K. S.; Mannermaa, E.; Turner, H.; Hakli, M.; Wolosin, J. M.; Tervo, T.; Honkakoski, P.; Urtti, A. *J Pharm Sci* 2010, **99**, 1087–1098.
100. Vellonen, K. S.; Hakli, M.; Merezhinskaya, N.; Tervo, T.; Honkakoski, P.; Urtti, A. *Eur J Pharm Sci* 2010, **19**, 241–247.
101. Xu, S.; Flanagan, J. L.; Simmons, P. A.; Vehige, J.; Willcox, M. D.; Garrett, Q. *Mol Vis* 2010, **16**, 1823–1831.
102. Rangasamy, S.; Srinivasan, R.; Maestas, J.; McGuire, P. G.; Das, A. *Invest Ophthalmol Vis Sci* 2011, **52**, 3784–3791.
103. Kashyap, M. V.; Ranjan, A. P.; Shankardas, J.; Vishwanatha, J. K. *In Vivo* 2013, **27**, 685–694.
104. Carter, A. M. *Physiol Rev* 2012, **92**, 1543–1576.
105. Kitano, T.; Iizasa, H.; Hwang, I. W.; Hirose, Y.; Morita, T.; Maeda, T.; Nakashima, E. *Biol Pharm Bull* 2004, **27**, 753–759.
106. Lager, S.; Powell, T. L. *J Pregnancy* 2012, **2012**, 179827.
107. Rytting, E.; Ahmed, M. S. Fetal Drug Therapy. In *Clinical Pharmacology During Pregnancy*; Mattison, D. R., Ed.; Elsevier: Amsterdam, 2013, 55–72.
108. Vahakangas, K.; Myllynen, P. *Br J Pharmacol* 2009, **158**, 665–678.
109. Sastry, B. V. *Adv Drug Deliv Rev* 1999, **38**, 17–39.
110. Prouillac, C.; Lecoeur, S. *Drug Metab Dispos* 2010, **38**, 1623–1635.
111. Avery, M. L.; Meek, C. E.; Audus, K. L. *Placenta* 2003, **24**, 45–52.
112. Rytting, E.; Bryan, J.; Southard, M.; Audus, K. L. *Biochem Pharmacol* 2007, **73**, 891–900.
113. Li, H.; van Ravenzwaay, B.; Rietjens, I. M.; Louisse, J. *Arch Toxicol* 2013, **87**, 1661–1669.

114. Koeppen, B. M.; Stanton, B. A. *Berne & Levy Physiology*, 6th ed.; Mosby Elsevier: Philadelphia, 2010.
115. Pandit, N. K. *Introduction to the Pharmaceutical Sciences*; Lippincott Williams & Wilkins: Baltimore, 2007.
116. Terryn, S.; Jouret, F.; Vandenabeele, F.; Smolders, I.; Moreels, M.; Devuyst, O.; Steels, P.; Van Kerkhove, E. *Am J Physiol Renal Physiol* 2007, **293**, F476–F485.
117. Markadieu, N.; San Cristobal, P.; Nair, A. V.; Verkaart, S.; Lenssen, E.; Tudpor, K.; van Zeeland, F.; Loffing, J.; Bindels, R. J.; Hoenderop, J. G. *Am J Physiol Renal Physiol* 2012, **303**, F886–F892.
118. Schlatter, P.; Gutmann, H.; Drewe, J. *Eur J Pharm Sci* 2006, **28**, 141–154.
119. Taub, M. *Methods Mol Biol* 2005, **290**, 231–247.
120. Vesey, D. A.; Qi, W.; Chen, X.; Pollock, C. A.; Johnson, D. W. *Methods Mol Biol* 2009, **466**, 19–24.
121. Van der Hauwaert, C.; Savary, G.; Gnemmi, V.; Glowacki, F.; Pottier, N.; Bouillez, A.; Maboudou, P.; Zini, L.; Leroy, X.; Cauffiez, C.; Perrais, M.; Aubert, S. *PLoS One* 2013, **8**, e66750.
122. Lash, L. H.; Putt, D. A.; Cai, H. *Toxicology* 2006, **228**, 200–218.
123. Jang, K. J.; Mehr, A. P.; Hamilton, G. A.; McPartlin, L. A.; Chung, S.; Suh, K. Y.; Ingber, D. E. *Integr Biol (Camb)* 2013, **5**, 1119–1129.
124. Volpe, D. A. *J Pharm Sci* 2008, **97**, 712–725.
125. Liang, M.; Ramsey, C. R.; Knox, F. G. *Kidney Int* 1999, **56**, 2304–2308.
126. Kobayashi, M.; Shikano, N.; Nishii, R.; Kiyono, Y.; Araki, H.; Nishi, K.; Oh, M.; Okudaira, H.; Ogura, M.; Yoshimoto, M.; Okazawa, H.; Fujibayashi, Y.; Kawai, K. *Nucl Med Commun* 2010, **31**, 141–146.
127. Chassin, C.; Bens, M.; Vandewalle, A. *Cell Biol Toxicol* 2007, **23**, 257–266.
128. Hara, C.; Satoh, H.; Usui, T.; Kunimi, M.; Noiri, E.; Tsukamoto, K.; Taniguchi, S.; Uwatoko, S.; Goto, A.; Racusen, L. C.; Inatomi, J.; Endou, H.; Fujita, T.; Seki, G. *Pflugers Arch* 2000, **440**, 713–720.
129. Jenkinson, S. E.; Chung, G. W.; van Loon, E.; Bakar, N. S.; Dalzell, A. M.; Brown, C. D. *Pflugers Arch* 2012, **464**, 601–611.
130. Glube, N.; Giessl, A.; Wolfrum, U.; Langguth, P. *Nephron Exp Nephrol* 2007, **107**, e47–e56.
131. Wieser, M.; Stadler, G.; Jennings, P.; Streubel, B.; Pfaller, W.; Ambros, P.; Riedl, C.; Katinger, H.; Grillari, J.; Grillari-Voglauer, R. *Am J Physiol Renal Physiol* 2008, **295**, F1365–F1375.
132. Astashkina, A. I.; Mann, B. K.; Prestwich, G. D.; Grainger, D. W. *Biomaterials* 2012, **33**, 4700–4711.
133. Elliott, N. T.; Yuan, F. *J Pharm Sci* 2011, **100**, 59–74.
134. Matsusaki, M.; Case, C. P.; Akashi, M. *Adv Drug Deliv Rev* 2014, **74**, 95–103.
135. Astashkina, A. I.; Mann, B. K.; Prestwich, G. D.; Grainger, D. W. *Biomaterials* 2012, **33**, 4712–4721.